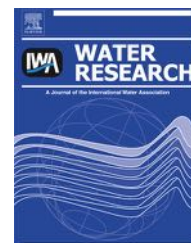


Available online at www.sciencedirect.com

ScienceDirect

journal homepage: www.elsevier.com/locate/watres

Automatic microfiber filtration (AMF) of surface water: Impact on water quality and biofouling evolution

Anat Lakretz^a, Hila Elifantz^b, Igor Kviatkovski^c, Gonen Eshel^d,
Hadas Mamane^{a,*}

^a School of Mechanical Engineering, Faculty of Engineering, Tel Aviv University, Tel Aviv 69978, Israel

^b Plant and Environmental Sciences, The Hebrew University of Jerusalem, Jerusalem, Israel

^c Institute of Soil, Water and Environmental Sciences, Agricultural Research Organization, PO Box 6, Bet Dagan, Israel

^d Amiad Water Systems, Amiad, Galil Elyon 12335, Israel

ARTICLE INFO

Article history:

Received 2 July 2013

Received in revised form

4 October 2013

Accepted 5 October 2013

Available online 16 October 2013

Keywords:

Biofilm

Water

Thread filtration

Microbial community composition

Particle size and circularity

ABSTRACT

In the current study we examined the impact of thread filtration using an automatic microfiber filter on Lake Kinneret water quality and as a new application to control biofouling over time. We found that automatic microfiber filtration (AMF) reduced total iron and aluminum in water by over 80%. Particle analysis (>2 μm) revealed a total particle removal efficiency of ~90%, with AMF removal efficiency increasing with increasing particle size and decreasing particle circularity. Regarding microbiological parameters, AMF did not affect bacterial counts or composition in the water. However, it did control biofilm evolution and affected its microbial community composition. AMF controlled biofilm over time by maintaining premature biofilms of less than 10 μm mean thickness compared to biofilms of unfiltered water (up to 60 μm mean thickness). In addition, biofilms developing in AMF filtered water contained relatively low levels of extracellular polymeric substances. While biofilms of unfiltered water were dominated by *Proteobacteria* (≤50%) followed by *Bacteroidetes* (20–30%) during all 4 weeks of the experiment, biofilms of AMF filtered water were dominated by *Proteobacteria* (≤90%) and especially *Alphaproteobacteria* after 2 weeks, and *Chloroflexi* (~60%) after 4 weeks. The decrease in *Bacteroidetes* might originate from removal of transparent exopolymer particles, which are occasionally colonized by *Bacteroidetes*. The increase in *Alphaproteobacteria* and *Chloroflexi* was explained by these robust groups' ability to adjust to different environments.

© 2013 Elsevier Ltd. All rights reserved.

1. Introduction

Biofouling is the undesirable deposition of microorganisms and their secretions (extracellular polymeric substances—EPS) on surfaces in aquatic environments, which in turn interferes with

the technical, economic, and hygienic requirements of water treatment (Flemming, 2002). Biofouling is ubiquitous in water systems, posing major problems in all of the systems' sectors. In drinking-water distribution systems biofouling can cause head losses, biocorrosion (Coetser and Cloete, 2005), water-

* Corresponding author. Tel.: +972 3 6408129; fax: +972 3 7334.

E-mail address: hadasmg@post.tau.ac.il (H. Mamane).

quality deterioration, development of odor and color, and potential health hazards (Momba et al., 2000). Typical factors affecting biofilm formation include the nature and concentration of biodegradable compounds in the water, the materials used for the drinking-water distribution system, and water temperature. Common treatments to prevent biofouling include barriers, such as minimizing nutrients in the feed, altering surface materials and using disinfectants (oxidative or UV irradiation) (Momba et al., 2000).

Processes that improve water quality, such as filtration, might also control factors that further impact biofouling in water systems. Filtration is a process that removes particles from suspension in water. Particles in water sources may be classified into various groups, such as living vs. nonliving, nano-sized vs. submicron- to micron-sized, and mineral vs. organic. Examples of living particles are bacteria, viruses, protozoa and algae, while nonliving particles include mineral and organic particles, cell debris and macromolecules. Particles in water sources may be dispersed as individual entities or associated in flocs or aggregates. Water treatment facilities generally employ granular-media or membrane filters prior to disinfection. Conventional treatment processes for surface water include coagulation, flocculation, sedimentation, granular media filtration and disinfection, with coagulation and flocculation serving to create conditions for subsequent removal of particulates and dissolved organic matter. With water of higher quality, direct and in-line filtration can be used. Another process might include a screening system, micro- or ultrafiltration (MF/UF) membranes followed by disinfection. Depth filtration is the dominant mechanism for granular filtration, where suspended particles are removed by attachment to the filter media or to previously retained particles which serve as additional collection sites for improved removal efficiency (Darby et al., 1992). Straining is the dominant mechanism in MF/UF-membrane filtration, where particles larger than the retention rating of the membrane collect at the surface. These filters usually do not require chemical conditioning of the particles, which may be an advantage over granular filtration. MF/UF-membrane filtration is independent of particle concentration in the feed and is more compact. However, membranes are subjected to particulate, dissolved organic or biological fouling, which affects design and operation.

The Amiad automatic microfiber filtration (AMF) technology has been characterized by Ityel (2011) and Eshel et al. (2012). In AMF process, feed water is filtered through multi-layered microfiber cassettes in a range of 2–20 μm depending on the application. Larger particles are blocked on the surface of the thread cassettes (as with straining mechanisms), while the finer particles penetrate the surface and are trapped deeper inside the multiple thread layers (as with depth filtration). Ityel (2011) noted that AMF's effective removal of oxidized iron particles gives it an advantage over granular filtration. This advantage was further emphasized by AMF's ability to overcome the growth of iron bacteria, which cause clumping of granular media particles and free flow of unfiltered water through the gaps created in the filter media. The filtration mechanics of AMF technology consist of a combination of surface and depth filtration leading to high filtration capacity in a compact package, which also includes a self-cleaning mechanism. Eshel et al. (2012) investigated the

application of AMF with Lake Kinneret water, paying particular attention to the impact of AMF on transparent exopolymer particles (TEP) and chlorophyll removal with respect to biofouling control. TEP are transparent sticky organic microgel particles which are ubiquitous in natural waters and are suspected to enhance biofilm formation in water systems (Berman, 2012). Eshel et al. (2012) concluded that AMF reduces TEP and chlorophyll in Lake Kinneret water, and is very efficient at controlling biofouling.

In the current study, our aim was to better understand this new application of AMF technology in terms of water quality and biofouling control over time. The specific objectives were to assess the impact of AMF on (1) water quality, including a comprehensive analysis of size and shape of the removed particles, and microbial count and community population, (2) biofouling evolution, using extensive weekly investigations of the biofilm's physical and compositional parameters.

2. Material and methods

2.1. Experimental setup

The pilot plant experimental setup is shown in Fig. 1 and described in detail in Eshel et al. (2012). Briefly, surface water from western Lake Kinneret (Sea of Galilee, Israel) was pumped at Kibbutz Ginosar and was either passed directly through a reference Robbins device or was first subjected to AMF (automatic microfiber filter, filtration grade 3 μm , Amiad Water Systems, Israel) and then passed through a second Robbins device (Fig. 1). The data presented herein were collected throughout 1 year of experiments—from February (winter) 2011 to February (winter) 2012. During this time, four biofouling experiments were conducted: (1) February 2011; (2) June 2011; (3) December 2011 and (4) January 2012. Every biofouling experiment lasted 4 weeks. Biofilm analyses were conducted at the start of the experiment and in the first, second, third and fourth weeks (T0, 1 W, 2 W, 3 W and 4 W, respectively). Water was collected on a weekly basis before filtration (BF) and after AMF filtration (AF) for physical and chemical analyses. Particle analysis, bacterial counts and community composition analyses were performed in some of the experiments to extend our understanding of the effect of AMF on water quality and biofouling control over time.

2.2. Amiad automatic microfiber filter

The components of the automatic microfiber filter and its mode of operation are described in detail in Ityel (2011) and

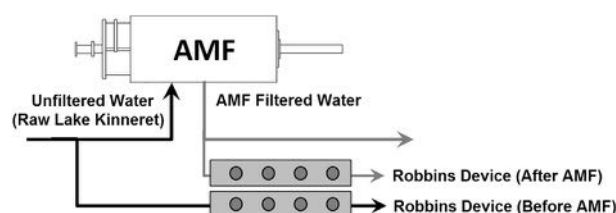


Fig. 1 – Pilot plant experimental setup.

Eshel et al. (2012). In principle, the filter's basic element is the thread cassette, which is a filter medium consisting of multiple layers of textile threads wound around a grooved rigid plastic plate. The thread type and tension and the number of layers define the degree of filtration, which can range between 2 and 20 μm . The cassettes are attached to a circular holder connected to a collector pipe, forming a unified package. These packages are attached to one another and form a complete cassette cartridge. The cartridge is then installed into the filter housing.

2.3. Water-quality analyses

2.3.1. Chemical analysis

Total iron and aluminum were measured with a VISTA-PRO inductively coupled plasma-optical emission spectrometer (ICP-OES; Varian, Australia) according to Standard Methods 3120B (APHA et al., 2005). Total Organic Carbon (TOC) and Dissolved Organic Carbon (DOC) were measured with a TOC-VCPN (Shimadzu, Japan) according to Standard Method 5310B High-Temperature Combustion Method.

2.3.2. Particle analysis

Particles suspended in liquid were analyzed by Micro Flow Imaging technology (DPA 4100, Protein Simple Inc., Canada, www.proteinsimple.com). This apparatus employs a digital camera with an illumination and magnification system to capture in-situ images of suspended particles in a flowing sample. Basically, a sample fluid is drawn through a flow cell and sections of the fluid are illuminated with a light-emitting diode light source at $\lambda = 470 \text{ nm}$, magnified and imaged onto a digital camera. These captured images are automatically analyzed to determine various size and shape parameters representing the two-dimensional projection of the particles.

Analysis was conducted on particles of between ~ 2 and $400 \mu\text{m}$. Pixel density was 1.3 Mega pixels, with a field of view of $1760 \times 1400 \mu\text{m}$ and a resolution of $0.25 \mu\text{m}$. The threshold value separating the background from the particles was defined automatically; during the run, particle images were obtained in binary and gray-scale files, with a predefined number of images captured for each run. System calibration was conducted with polymer microspheres with mean diameters of $5 \mu\text{m} \pm 0.05 \mu\text{m}$ and $10 \mu\text{m} \pm 0.1 \mu\text{m}$ and narrow size distributions, as certified by the manufacturer (Duke Scientific, USA). The geometric characteristics of the samples were expressed in the following parameters: (1) ECD (μm) – equivalent circular diameter of an object, which represents the diameter of a sphere that occupies the same two-dimensional surface area as the particle; (2) circularity – a dimensionless number between 0 and 1, where circularity = 1 for a spherical particle and 0 for a nonspherical one. It is defined as (circumference of an equivalent area circle)/(perimeter of the particle). Knowledge of the concentration of particles before and after filtration allows us to calculate the removal efficiency of the AMF filter. Percent relative removal efficiency (% RRE) was calculated using Eq. (1), where C_i is the particle concentration of unfiltered Lake Kinneret water and C_o is the particle concentration in the AMF filtered water. To determine removal, C_i was sampled simultaneously with C_o .

$$\% \text{ RRE} = \left(\frac{C_i - C_o}{C_i} \right) \cdot 100 \quad (1)$$

2.3.3. Bacterial counts

Total bacterial counts in unfiltered and AMF filtered water were determined by 4',6'-diamidino-2-phenylindole (DAPI). A 25-ml sample of the water was filtered through a $0.2\text{-}\mu\text{m}$ polycarbonate membrane (GE Water and Process Technologies, USA). The membrane was then cut into 16 equal pieces and each filter piece was stained with $0.5 \text{ ng}/\mu\text{l}$ DAPI. Images were collected using a Leica SP5 confocal microscope and counted using Daim software (Daims et al., 2006).

2.4. Microbial community composition in water and in biofilm

For microbial community composition analysis, samples of the planktonic community were collected by filtering 200 ml of water (unfiltered or AMF filtered) through a $0.2\text{-}\mu\text{m}$ polycarbonate membrane for phylogenetic affiliation analysis using 16S rRNA gene pyrosequencing. For biofilm community composition, glass coupons were gently removed from the biofilm device on site and placed in a 15-ml Falcon tube. All samples for DNA extraction were stored at -80°C until further processing. DNA extraction was performed using the Ultra-Clean soil DNA isolation kit (MoBio Laboratories, USA) with minor modifications to the initial step for the biofilm samples. Sterile glass beads and 1 ml extraction buffer were added to the tubes containing the glass coupons. The tubes were vigorously vortexed for 10 min and then centrifuged at $4,000g$ for 15 min. Supernatants were transferred to 1.5-ml microcentrifuge tubes, and the rest of the extraction process was performed according to the manufacturer's instructions. The extracted DNA was sent for pyrosequencing analysis to the Research and Testing Laboratory (Lubbock, TX, USA) using the 27F primer (Lane, 1991). The data retrieved from the pyrosequencing analysis were analyzed using Mothur (Schloss et al., 2009).

2.5. Biofilm formation in Robbins devices

Biofilm evolution over time was measured using two Robbins devices through which unfiltered water (Robbins device before AMF) and AMF filtered water (Robbins device after AMF) were passed (Fig. 1). Flow rates of $0.5 \text{ m}^3/\text{h}$ and velocities of 0.2 m/s were maintained throughout the experiments. The Robbins devices were made of 1" PVC pipes with parallel ports. Each port held a press-fit plug holding a glass sample coupon with a surface area of 50 mm^2 . The surface area of the coupon was designed to be part of the device's channel wall and exposed to the flowing unfiltered or filtered water.

The Robbins devices allowed simulation of flow conditions similar to those of drinking-water distribution systems. Algae, bacteria, organic and inorganic material that were present in the water could adhere to the glass coupons and eventually formed biofilms. Glass coupons were aseptically removed every week from both Robbins devices for microscopy and molecular analyses.

2.6. Biofilm analysis using microscopy techniques

2.6.1. Determination of biofilm structure parameters by confocal laser scanning microscopy (CLSM)

Biofilm structural characteristics were determined by staining for bacterial cells (nucleic acids) with SYTO[®]9 (Invitrogen-Molecular Probes, USA) and for EPS polysaccharides with concanavalin A (Invitrogen-Molecular Probes, USA) as outlined by Strathmann et al. (2002) and detailed by Eshel et al. (2012). CLSM was performed with a Leica SP5 confocal microscope. For SYTO9, excitation was determined at 488 nm and emission between 495 and 537 nm. Concanavalin A was determined at 561 nm excitation with emissions at 570–620 nm. For each sample, 15 fields of view were taken with a field size of 164 × 164 μm. Quantitative image analyses were performed with PHLIP software (Mueller et al., 2006). Three-dimensional representations of CLSM image stacks were generated using IAMRIS software (Bitplane Scientific Software, USA) in volume-rendering mode.

2.6.2. Visualization of biofilm morphology by scanning electron microscopy (SEM)

Surface morphology of the biofilm samples that developed on glass coupons in the Robbins devices were imaged by means of an environmental SEM (Quanta 200 field emission gun from FEI, USA) operated in high-vacuum mode. The glass coupons were prepared by fixation in 4% paraformaldehyde, air-drying overnight and gold-palladium coating before imaging.

3. Results and discussion

The impact of AMF on water-quality parameters was determined by comparing unfiltered and AMF filtered water after different weekly periods. The examined water parameters were TOC, DOC, iron and aluminum removal, particle size and shape, bacterial counts and microbial community composition. The impact of AMF on biofilm evolution was examined using Robbins devices located before and after the AMF filter, with a focus on biofilm thickness, EPS biovolume, SEM imaging and biofilm microbial community.

3.1. Impact of AMF on water quality

3.1.1. Water-quality parameters

Water was collected on a weekly basis before and after AMF for physical and chemical analyses. Total organic carbon in the unfiltered and AMF filtered water was 2.9 ± 0.2 mg/l and 2.8 ± 0.1 mg/l, respectively; dissolved organic carbon was 2.7 ± 0.1 mg/l for both types of water. It could therefore be concluded that most of the organic carbon in Lake Kinneret water is in its dissolved form and is not likely to be filtered by the AMF technology. Eshel et al. (2012) showed ~90% removal of turbidity, >3-μm particles and chlorophyll. They attributed their results to the fact that planktonic algae (which can be indirectly evaluated by chlorophyll amounts) are probably the main source of turbidity and the >3-μm particles in Lake Kinneret water, and are efficiently removed by AMF. Regarding removal percentages of total suspended solids and TEP, Eshel et al. (2012) obtained lower results (~70% and

~50%, respectively), explained by the high proportion of small-sized (<3 μm) particulate matter normally present in Lake Kinneret. This particulate matter can be either nanophytoplankton populations (which would account for the chlorophyll fraction that passed through the AMF) or colloidal precursors of TEP, which are not expected to be removed by AMF filtration.

TEP have been acknowledged as a critical factor in biofilm formation in filtration processes (Bar-Zeev et al., 2012b; Berman, 2012). TEP removal has been evaluated in various treatments. For example, Bar-Zeev et al. (2012a) found that application of rapid sand filtration leads to TEP removal that varies from ~20 to 90%. The variation was related to the TEP/EPS being sloughed off from mature biofilm and, at the same time, being degraded by bacteria. A study by Villacorte et al. (2009) revealed that ultrafiltration pretreatment for Reverse Osmosis (RO) systems is most efficient at removing particulate TEP (>0.4 μm), while microfiltration or coagulation followed by sedimentation and rapid sand filtration only partially removed it. None of the pretreatments totally removed colloidal TEP (0.05–0.4 μm).

Other parameters that were reduced by AMF were total iron (μg/l) and total aluminum (μg/l), with about 80% removal (Table 1). These results are in accordance with Ityel (2011) who introduced AMF as an alternative filtration technology for the removal of iron from water preconditioned with aeration. That author emphasized the advantage of the self-cleaning AMF over sand-media filtration in its ability to overcome the growth of iron bacteria, due to the nature of the cassette's structure, and thus avoid the consequent drop in filtration quality and bacteria thriving on unclean bedding. In addition, cationic metals (e.g. iron and aluminum) can promote and stabilize gel-like TEP formation through neutralization of negatively charged TEP precursors and cationic-bridge formation (Passow, 2002). Thus, removal of iron and aluminum may also support lower TEP levels in the AMF filtered water. In general, the issue of metal removal by thread filtration using AMF filter is still under investigation and requires further research. In order to better understand the removal mechanism it is suggested to analyze separately the fate of each

Table 1 – Total iron and aluminum concentrations (μg/l) before (BF) and after (AF) AMF filtration. T0, 2 W, and 4 W represent sampling times at the initiation of the experiment and 2 and 4 weeks into the experiment, respectively (February 2011).

Time	Iron total (μg/l)			Aluminum (μg/l)		
	BF	AF	% Removal	BF	AF	% Removal
T0	90	15 ^a	83%	78	13 ^a	83%
2 W	125	22 ^a	82%	135	12 ^a	91%
4 W	114	21 ^a	82%	72	13 ^a	82%
Average	110	19 ^a	82%	95	13 ^a	85%

^a Total iron and aluminum concentrations obtained after AMF filtration were very close to the lower threshold of the ICP quantification method. The deviations between replicates are known (20% for μg/l values). Nevertheless, it is apparent that the removal percentages of both total iron and aluminum are significant and estimated to be ~80% and ~85%, respectively.

metal phase (e.g. particulate or dissolved). Oxidation of soluble metals such as iron, manganese and aluminum can form precipitates that can be removed by the AMF. It can be assumed that the iron and aluminum removed in the current study were mostly of particulate characteristics. It is presumable that some of the iron and aluminum removed were integrated in TEP and were removed with it.

3.1.2. Particle removal

Turbidity is the most common parameter used to monitor particles. Both turbidity and total suspended solids (TSS) are parameters representing scattering or weight of particles, however, they do not provide information on their size, shape, or concentration and thus may not be the best measure of particle-removal efficiency. To extend our understanding of AMF efficiency, dynamic image analysis of particles was conducted. Dynamic image analysis is a rapid and sensitive technique to characterize particle size, shape, count and transparency (see Section 2.3.2).

Table 2 shows %RRE as a function of ECD range (four separate analyses conducted in December 2011 and January 2012) and an example of particle concentrations before (BF) and after (AF) AMF (4 W, January 2012). BF and AF particle concentrations decreased with increasing ECD. In general, both filtered and unfiltered Lake Kinneret water contained mainly smaller (<3 μm) particulate matter. In addition, AMF removal efficiency (%RRE) generally increased with increasing ECD range (Table 2). The average particle removal of AMF for December 2011 and January 2012 was $86 \pm 8\%$, with removal efficiencies of $95 \pm 4\%$ for particles >3 μm , $85 \pm 0.5\%$ for particles $\leq 5 \mu\text{m}$, $91 \pm 3\%$ for 5–10 μm particles, and $97 \pm 2\%$ for particles of $\geq 10 \mu\text{m}$. Eshel et al. (2012) also found $93 \pm 4\%$ removal of >3- μm particles in Lake Kinneret water using an AccuSizer particle counter. In summary, as expected, AMF did not remove smaller particles (e.g. colloids, viruses, and bacteria). However, AMF removal efficiency increased gradually with increasing particle size (e.g. larger bacteria, bacterial flocs, organic debris, algae, cysts, silt, and sand).

Particle image analysis can potentially serve to evaluate treatment-process efficiencies, such as addition of coagulants to granular filtration, by coupling size and shape parameters

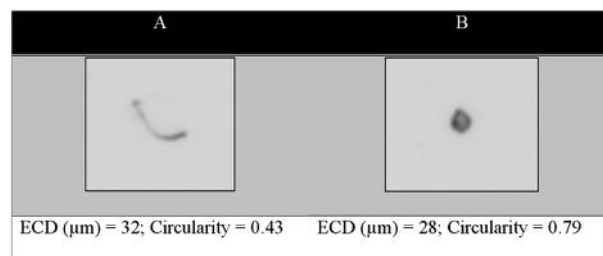


Fig. 2 – Example of two similar-sized particles with different circularity values. ECD, equivalent circular diameter.

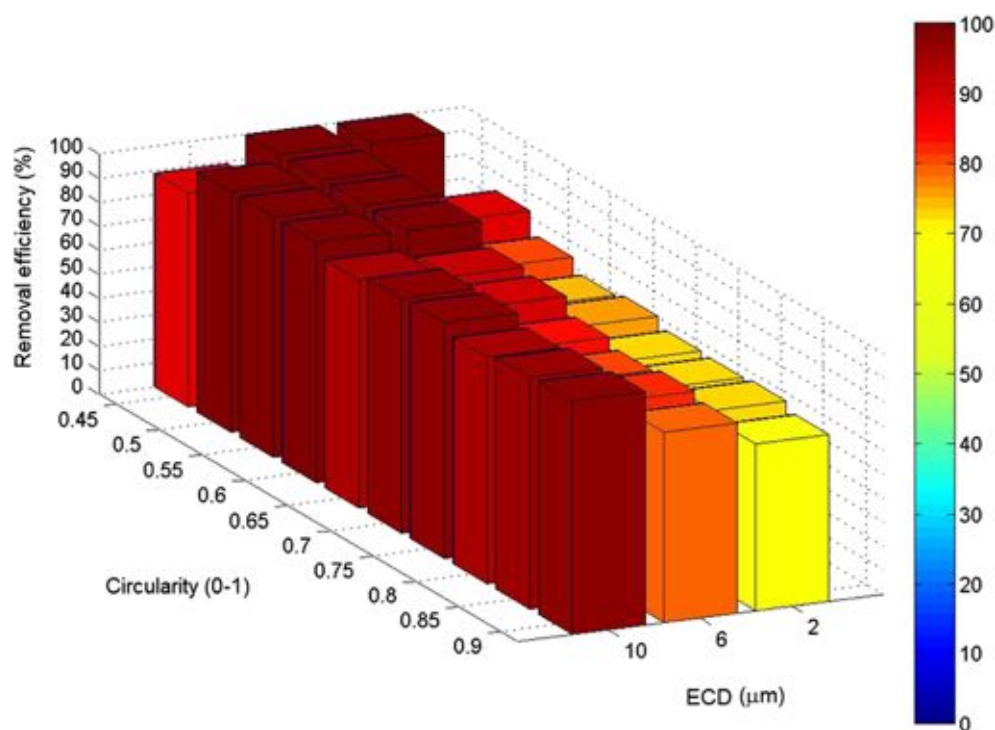
into a meaningful tool. The efficiency of AMF in removing differently shaped particles has never been investigated – removal efficiency is usually evaluated by analyses of size, not shape. The circularity of a particle defines how close it is to a circle, with a value of 1 representing a perfect circle, and zero representing an irregular, needle-shaped particle (Section 2.3.2). The shapes of the natural particles in the Lake Kinneret water were expected to be complex and variable. Fig. 2 illustrates two similar-sized particles (~30 μm) with different circularity values. The elongated banana like particle (Fig. 2A) had a circularity value of 0.43, while the rounded particle (Fig. 2B) had almost double the value, 0.79. Percent RRE as a function of circularity might depend on particle size since the perimeter of a particle depends on its resolution, and resolution depends on, among other things, size. For example, larger particles and finer resolution result in more accurate measurements. To avoid this effect, circularity data were analyzed in size ranges.

Fig. 3 illustrates %RRE as a function of both circularity and ECD ranges (4 W, January 2012). Measurements in other periods gave similar trends (data not shown). In general, %RRE of AMF increased with decreasing particle circularity. In addition, the aforementioned increase in %RRE with particle size was verified graphically. Particles of all sizes with circularity <0.6 were almost completely removed, whereas particles with circularity between 0.6 and 0.9 showed a trend of decreased removal with increasing circularity, which was more significant for the smaller particle sizes (<10 μm) (Fig. 3). These results are remarkably similar to those obtained by Mamane et al. (2008) when examining granular filtration without coagulants. These authors found enhanced removal of particles >10 μm with low circularity (<0.6). Addition of polyaluminum chloride resulted in higher removal efficiencies for all particles sizes at all circularity values.

Mamane et al. (2008) observed spikes when plotting percent particle removal by granular filtration as a function of ECD. This was because the structures of the deposits accumulated on the filter are not equally strong, and under the hydrodynamic forces of flow, these structures may be partially destroyed and cause the disintegration of previously fixed flocs (Mintz, 1966). In addition, Ives (1982) found that floc detachment or particle break-off might occur and impact particle effluent morphology over time. Ives (1982) concluded that the hydrodynamic mechanism for particle transport to the filter is related to particle shape. Mamane et al. (2008)

Table 2 – %RRE as a function of ECD ranges (T0 and 3 W in December 2011; 1 W and 4 W in January 2012). The 4 W time point in January 2012 includes particle concentrations before (BF) and after (AF) AMF filtration.

ECD (μm)	December 2011		January 2012			
	T0	3 W	1 W	4 W		
	% RRE	% RRE	%RRE	Particle conc. BF	Particle conc. AF	%RRE
2–3	96	80	88	26,894	6875	74
3–5	95	85	81	13,899	3034	78
5–10	94	91	84	5682	589	90
10–15	97	96	88	757	26	97
15–30	99	98	95	267	2	99
30–50	100	98	88	38	–	100
100+	100	100	100	6	–	100
Total	96	83	86	47,543	10,526	78



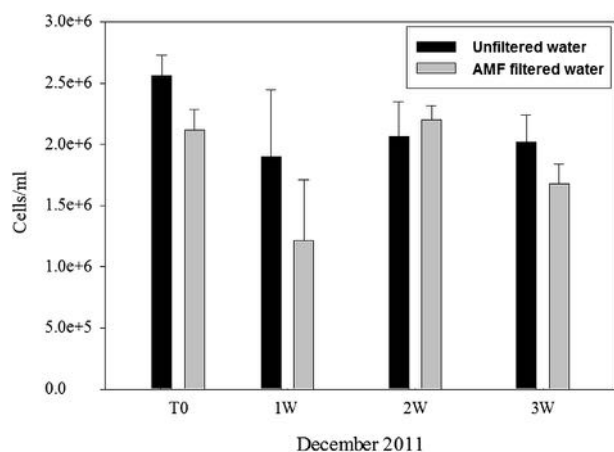


Fig. 4 – Bacterial counts in unfiltered (black) and AMF filtered (gray) water (December 2011). T0, 1 W, 2 W, and 3 W represent sampling times at initiation of experiment and 1, 2, and 3 weeks into experiment, respectively.

caused a change in the microbial community composition of the water. However, pyrosequencing analysis of the 16S rRNA gene as a phylogenetic marker suggested that only minor changes in microbial community composition occurred between the unfiltered and AMF filtered water (Fig. 5). In February 2011 (first biofilm experiment), we took a sample for microbial community composition analysis. The microbial community was composed of about 40% *Proteobacteria*, with predominantly *Alphaproteobacteria*, followed by *Beta*- and *Gammaproteobacteria*. The second dominant phylogenetic group was *Actinobacteria*, making up 15–30% of all bacteria, followed by *Bacteroidetes* (11–27%). These findings were in accordance with other freshwater microbial communities in, for example, freshwater marsh

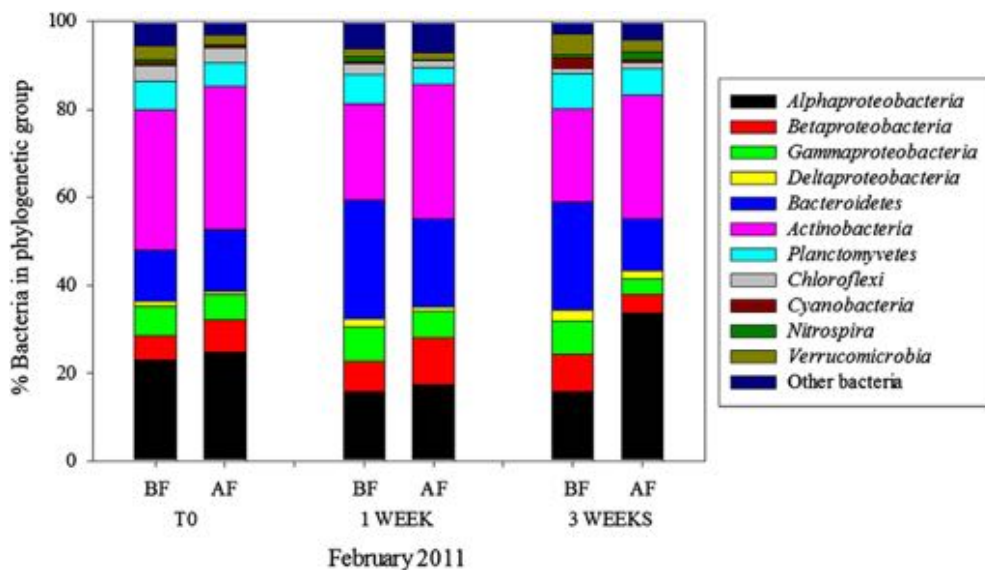


Fig. 5 – Microbial community composition before (BF) and after (AF) AMF filtration (February 2011). Sampling time is indicated in weeks. The *Proteobacteria* family was divided into the subgroups *Alpha*-, *Beta*-, *Gamma*-, and *Deltaproteobacteria*.

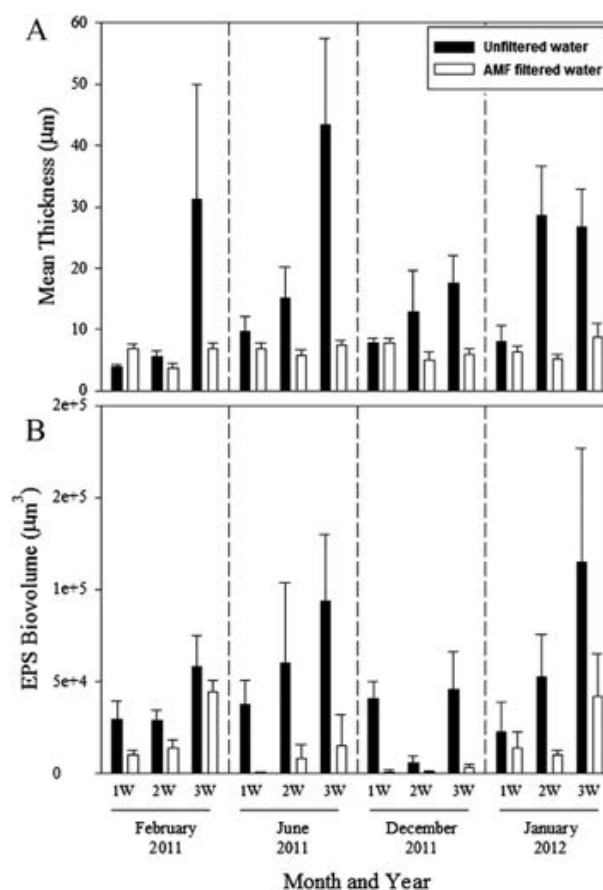


Fig. 6 – Mean thickness (A) and EPS biovolume (B) of biofilm formed in unfiltered (black) and AMF filtered (white) water. Analyses were performed for three weeks (1 W, 2 W, and 3 W) for each of the four experimental sets.

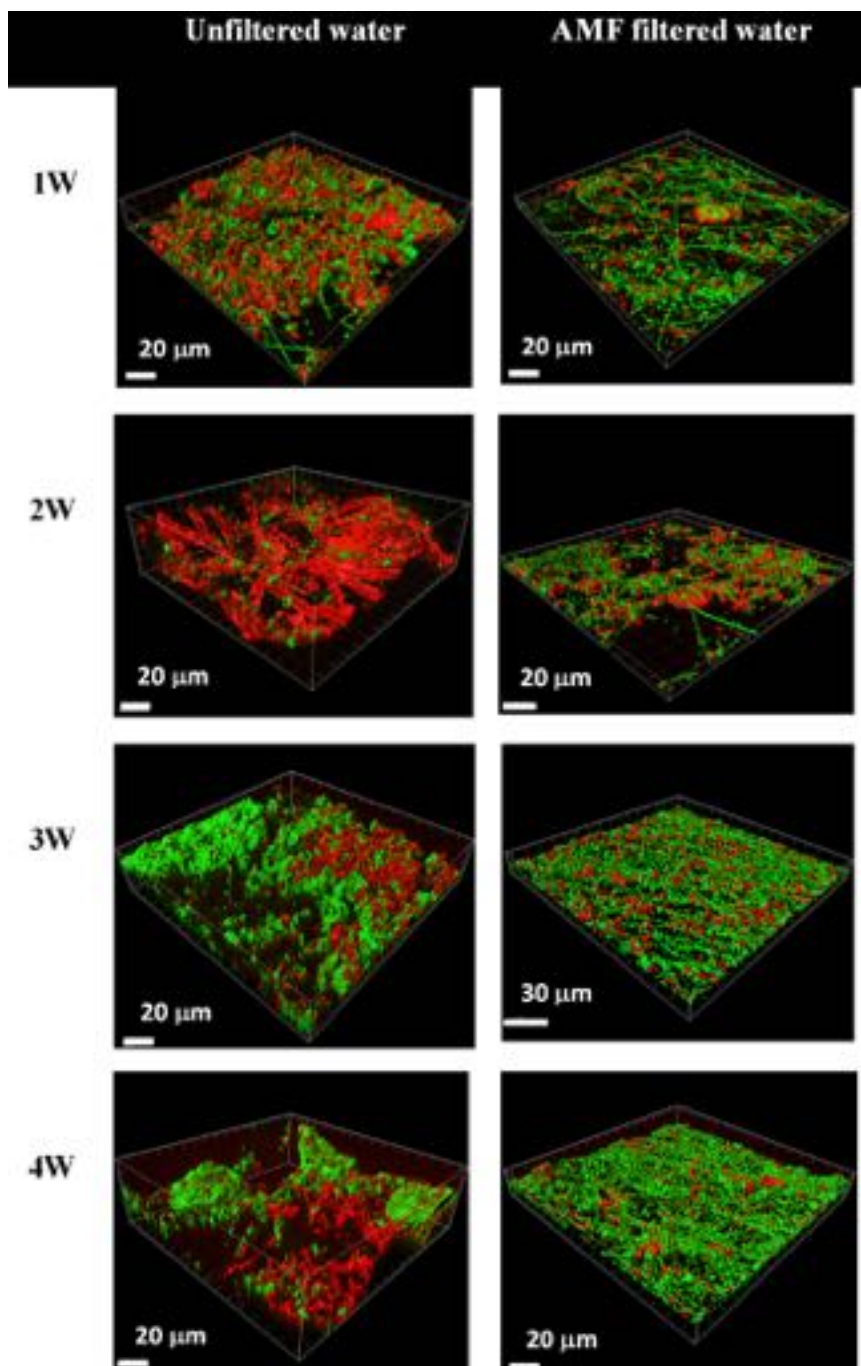


Fig. 7 – Representative IMARIS images of biofilm evolution in unfiltered (left) and AMF filtered (right) water (January 2012). Analyses were performed for 4 weeks of the experiment: 1 W, 2 W, 3 W and 4 W. Green: biomass; red: EPS.

microhabitats (Buesing et al., 2009), and with a recent global survey (Barberán and Casamayor, 2010).

3.2. Impact of AMF on biofouling control over time

Eshel et al. (2012) presented AMF as a good potential pre-treatment strategy for control of biofouling. The current research examined the effect of AMF on weekly biofouling evolution at higher resolution, using CLSM, SEM and community composition analysis.

3.2.1. Biofilm evolution (CLSM)

To assess AMF efficiency with respect to biofouling evolution, biofilm parameters such as mean thickness and EPS biovolume were measured over time (Fig. 6). Similar trend was noticed for all experiments. While the biofilm mean thickness increased with time in the unfiltered water, biofilm mean thickness with the AMF filtered water did not change significantly (Fig. 6A). A slightly different trend could be observed for EPS biovolume (Fig. 6B). In most cases, EPS biovolume increased with time with both water types. However, this

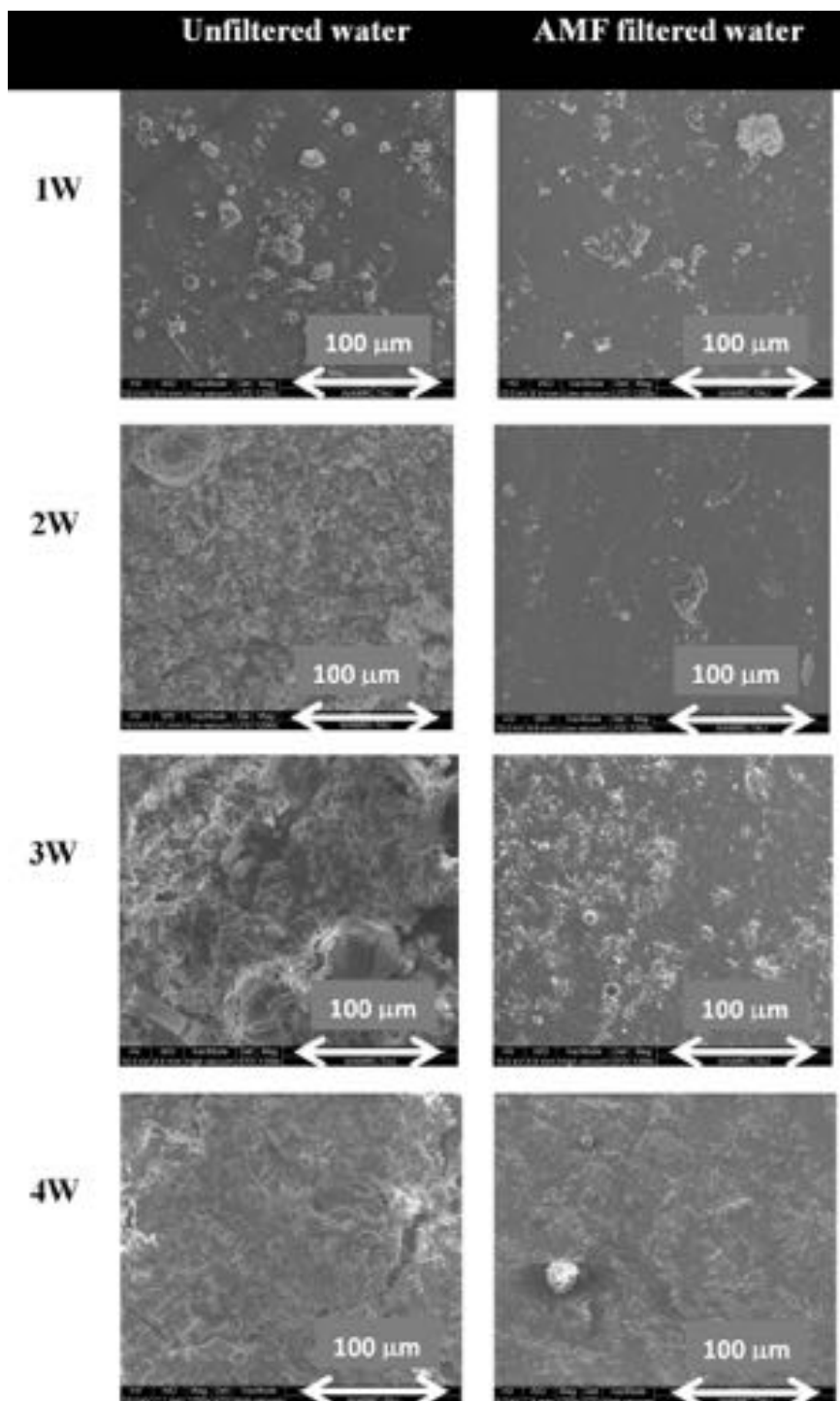


Fig. 8 – Representative SEM images of biofilm evolution in unfiltered (left) and AMF filtered (right) water (December 2011). Analyses were performed for 4 weeks of the experiment: 1 W, 2 W, 3 W and 4 W. Magnification: 1200X.

increase was much more significant with the unfiltered water than with the AMF filtered water. In addition, the increase in EPS biovolume in the AMF filtered water was not gradual; rather, it occurred between weeks 2 and 3 (from 40 to 80%).

Visualizing the CLSM results using IMARIS image analysis (Fig. 7, representative images from January 2012, fourth biofilm experiment) showed that the biofilm with the unfiltered

water reached maturity (a thick film full of biomass and EPS) after 2 weeks of growth (Figs. 7 and 2 W unfiltered water). In comparison, biofilms with the AMF filtered water did not mature to this extent, even after 4 weeks of growth (Figs. 7 and 4 W AMF filtered water). In addition, the biofilms developed in unfiltered water contained much more EPS, which was detectable at earlier stages compared to the biofilms

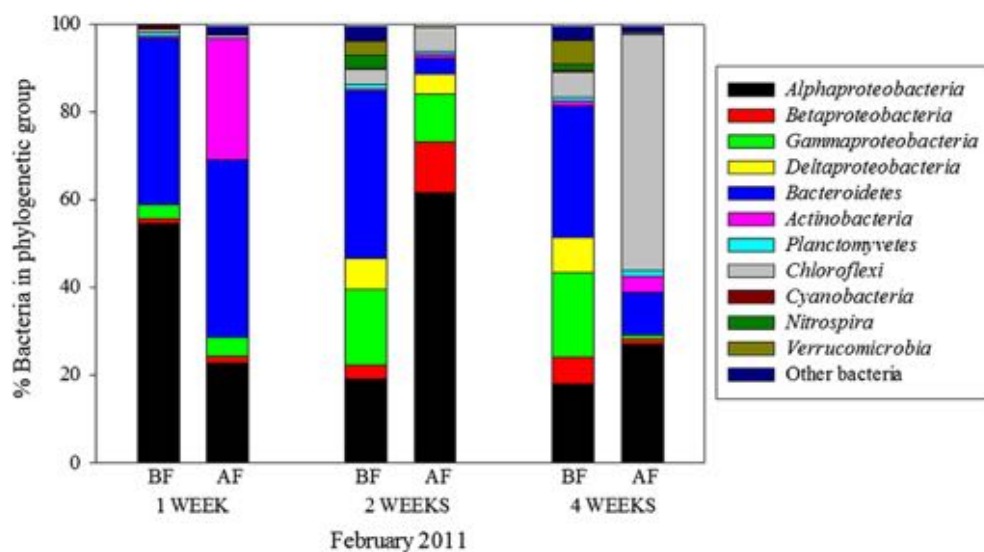


Fig. 9 – Microbial community composition in biofilm developed before (BF) and after (AF) AMF filtration. Biofilm age is indicated in weeks. The *Proteobacteria* family was divided into the subgroups *Alpha*-, *Beta*-, *Gamma*-, and *Deltaproteobacteria*.

developed in AMF filtered water (Fig. 7, in red). Berman et al. (2011) investigated the relationship between TEP levels in Lake Kinneret water and membrane clogging. These authors found that most of the EPS discovered at early stages on membranes originated from TEP (“planktonic EPS”) in the feed water rather than from EPS excreted by active bacteria attached to the surface. Similar results were obtained by Bar-Zeev et al. (2009a) who investigated TEP involvement in seawater membrane fouling. Thus, one of the plausible reasons for the lower EPS found in biofilms developed in AMF filtered water is the removal of TEP like particles. Lower EPS levels can contribute to biofouling inhibition, together with AMF removal of particles, nutrients, and microorganisms.

3.2.2. Biofilm evolution (SEM)

SEM analysis was conducted to assess surface morphology of the biofilms, and visualize some of their microbial inhabitants. Fig. 8 shows representative SEM images from December 2011 (third biofilm experiment). Once again, the biofilm of the unfiltered Lake Kinneret water was already mature after 2 weeks, and continued growing with time (Fig. 8, unfiltered water). These biofilms were highly diverse, containing phytoplankton such as dinoflagellates (e.g. *Peridinium*), diatoms (e.g. *Navicula* and *Cyclotella*), bacteria, and EPS (Prof. Berman, personal communication). Indeed, according to the Annual Report of the Kinneret Limnological Laboratory (KLL, 2011), the diatom population peaked in November of that year. Diatoms such as *Cyclotella* and *Discostella stelligera* were observed in November–December 2011. In addition, the end of 2011 was characterized by a *Peridinium* bloom, which continued until the beginning of 2012 (KLL, 2011). In contrast to biofilms with unfiltered water, the biofilms that developed in AMF filtered water were barely mature at 4 weeks (Fig. 8, AMF filtered water). Although showing some diversity of microbial species (e.g. *Cyclotella*, algae, and bacteria) and EPS at that time point, biofilms of AMF filtered water exhibited much

lower densities of material compared to biofilms of unfiltered water.

Algal involvement in biofouling has been investigated in several studies (Babel and Takizawa, 2010; Bar-Zeev et al., 2012b; Berman, 2012; Lee et al., 2006). Babel and Takizawa (2010) showed that algae can cause significant membrane fouling. Those authors stressed that algal fouling is quite complex due to the extracellular organic matter released by the cells, which significantly increases membrane resistance. Indeed, Lee et al. (2006) found that intercellular and/or extracellular algal and bacterial (e.g. cyanobacteria) organic matter can cause severe membrane fouling. In addition, algal and bacterial secretions and gelatinous envelopes surrounding phytoplankton can also form TEP in water (Berman, 2012). Thus, the lower EPS found in biofilms developed in AMF filtered water could also be a result of removal of bacteria (mostly attached to particles), algae and phytoplankton which tend to secrete EPS.

The current results show that AMF is effective in filtering Lake Kinneret water and most likely removes abiotic (e.g. sand, silt) and biotic (e.g. planktonic algae, microbial flocs, organic debris) particles and presumably also TEP/EPS/extracellular organic matter. All of these results can explain the high effectiveness of AMF in controlling biofouling evolution. This new application of biofouling control by AMF filtration could be applied to various water types. For example, in the operation of seawater RO (SWRO) desalination plants, where biological and organic fouling is a major problem (especially during algal bloom), AMF can be integrated in the process train to reduce the biofilm growth potential of the water. In this water type, AMF can be applied after preliminary screening as either a substitution for granular filtration or for cartridge filtration at the last stage of pretreatment before RO. In the first application, coagulants may be used in order to improve removal efficiencies. This application can be advantageous in places where there is a lack of area. The last application can be

applied also in brackish water RO (BWRO) desalination plants. In addition, according to pilot studies, AMF can be used as a tertiary treatment of effluents while controlling biofouling and removing Helminthes, *Giardia* and *Cryptosporidium* and for removal of precipitated phosphorus (unpublished data). In greenhouse irrigation systems, AMF can be used to remove Nematodes and to reduce turbidity before UV disinfection (unpublished data). In summary, AMF has a high potential as a biofouling control strategy in many applications and water types.

3.2.3. Biofilm microbial community composition over time before and after AMF filtration

In addition to the structural changes in the biofilm formed after AMF filtration, a change in microbial community composition was observed during the first biofilm experiment (Fig. 9). The 1-week-old biofilms were characterized by relatively low diversity (Shannon Index 2.8 and 2.3 for the biofilm formed in unfiltered and AMF filtered water, respectively, compared to diversity indexes of 5.2–5.4 in the biofilm formed in the unfiltered water at later stages of the experiment), and the dominant bacterial groups (*Alphaproteobacteria* and *Bacteroidetes*) were present in the biofilm of both the unfiltered and AMF filtered water (Figs. 9 and 1 W). However, the percentage of *Alphaproteobacteria* was lower, concomitant with a higher percentage of *Actinobacteria* in the biofilm formed in AMF filtered water (Figs. 9 and 1 W). The microbial communities of the biofilm formed in the unfiltered water after 2 and 4 weeks were similar to each other, with *Proteobacteria* making up 50% of the community, followed by *Bacteroidetes* at 20–30%. However, the microbial communities in the counterpart AMF filtered water samples were dominated by *Proteobacteria* (up to 90% of the community with a dominance of *Alphaproteobacteria*) at 2 weeks and *Chloroflexi* (~60%) at 4 weeks. In both cases, *Bacteroidetes* appeared to be less abundant in the biofilm formed in the AMF filtered water relative to that from the unfiltered water. In addition, the overall diversity differed between the two types of biofilm – decreasing from 5.4 and 5.4 in the unfiltered water to 2.6 and 2.5 in the AMF filtered water after 2 and 4 weeks, respectively.

As such temporal dynamics have never been studied before, explaining our results was a challenge. While the microbial community composition of the biofilm formed in the unfiltered water was relatively stable over time, that of the community after AMF filtration changed from one week to the next. From the second week of the experiment, there was an apparent decrease in the fraction of *Bacteroidetes* in the biofilm formed in AMF filtered water. This decrease corresponded to the decrease of this phylogenetic group in the AMF filtered water (Fig. 5) and in TEP concentration after filtration (Eshel et al., 2012). Bar-Zeev et al. (2012b) introduced a new term, protobiofilm, to describe those parts of the TEP that are heavily colonized by bacteria and other microorganisms. It has been already noted that *Bacteroidetes* are abundant on particles (Selje and Simon, 2003), and it is very likely that some of the *Bacteroidetes* in the feed water were attached to the TEP and therefore removed from the water, and as a result from the biofilm as well. The dramatic increase in *Alphaproteobacteria* in the second week could be explained by this group's ability to adjust to environments with low nutrient availability

(Newton et al., 2011; Nishimura and Nagata, 2007). Although there was almost no change in most of the parameters measured (Eshel et al., 2012), the decrease in iron and aluminum concentration suggests an overall shift in nutrient availability. Another dramatic change was observed after 4 weeks, with the dominance of *Chloroflexi* in biofilm formed in AMF filtered water. *Chloroflexi* can be found in a variety of environments and seem to be a robust phylogenetic group (Yamada and Sekiguchi, 2009) that can adjust to a variety of conditions. In one study, it was found that *Chloroflexi* could efficiently utilize degradation products (detritus) of other bacteria that colonized membrane filters (Miura and Okabe, 2008). This may suggest that in the case of the current study, *Chloroflexi* might be utilizing small-sized byproducts of other organisms which passed through the AMF filter or even originated from it with time.

4. Conclusions

- AMF of Lake Kinneret water impacted its quality by reducing total iron (~80%) and aluminum (~85%) contents. In addition, its particle removal efficiency was $86 \pm 8\%$ and increased with increasing particle size and with decreasing particle circularity.
- AMF controlled biofilm over time by maintaining premature biofilms of less than 10 μm mean thickness compared to biofilms of unfiltered water (up to 60 μm mean thickness). In addition, biofilms that developed in AMF filtered water contained much lower EPS levels than biofilms of unfiltered water.
- Although AMF did not affect bacterial counts or composition in the water, it did affect the microbial community composition of the biofilms. Biofilms that developed in AMF filtered water were dominated by different bacteria (*Proteobacteria* and especially *Alphaproteobacteria* after 2 weeks and *Chloroflexi* after 4 weeks) compared to biofilms of unfiltered water (predominantly *Proteobacteria* followed by *Bacteroidetes*).
- In summary, AMF exhibited stable operation and biofouling control over time. Thread filtration technologies that are dominated by a straining mechanism, such as AMF, usually do not require chemical conditioning of the particles, which can save on operational costs. Thus, a thorough understanding of AMF performance can provide designers and operators with means for improving filtration performance.

Acknowledgments

We greatly acknowledge Mr. Yigal Weinberger for excellent technical assistance in the particle analyses, Dr. Zahava Bar-kay from Tel Aviv University Center for Nanoscience and Nanotechnology for her kind assistance in the SEM analyses, Adam Blum from Amiad Water Systems for the dedicated field work, Adva Zach Maor from Amiad Water Systems for fruitful comments, and Dr. Liliya Simkhovitch from Mekorot Israel's National Water Company for her help with the water chemistry analyses. This work was supported by grants from the

Mayim Consortium, Magnet Programs, Office of the Chief Scientist, Israel Ministry of Industry, Trade and Labor. This research is part of Ms. Anat Lakretz's Ph.D. thesis, which is supported by a scholarship from the Israeli Water Authority and Ministry of Science and Technology.

We would like to specially acknowledge the contribution of Prof. Tommy Berman, who recently passed away under tragic circumstances, for his help with the phytoplankton identification and TEP information. Prof. Berman is regarded to be the developer of the transparent exopolymer particle (TEP) theory and their involvement in the formation of biofilm and membrane biofouling.

REFERENCES

- APHA (American Public Health Association), AWWA (American Water Works Association), Water Environment Federation (WEF), 2005. *Standard Methods for the Examination of Water and Wastewater*, twenty-first ed. (Washington, DC).
- Babel, S., Takizawa, S., 2010. Microfiltration membrane fouling and cake behavior during algal filtration. *Desalination* 261 (1–2), 46–51.
- Barberán, A., Casamayor, E.O., 2010. Global phylogenetic community structure and β -diversity patterns in surface bacterioplankton metacommunities. *Aquat. Microb. Ecol.* 59, 1–10.
- Bar-Zeev, E., Belkin, N., Liberman, B., Berman, T., Berman-Frank, I., 2012a. Rapid sand filtration pretreatment for SWRO: microbial maturation dynamics and filtration efficiency of organic matter. *Desalination* 286, 120–130.
- Bar-Zeev, E., Berman-Frank, I., Girshevitz, O., Berman, T., 2012b. Revised paradigm of aquatic biofilm formation facilitated by microgel transparent exopolymer particles. *Proc. Natl. Acad. Sci.* 109 (23), 9119–9124.
- Bar-Zeev, E., Berman-Frank, I., Liberman, B., Rahav, E., Passow, U., Berman, T., 2009a. Transparent exopolymer particles: potential agents for organic fouling and biofilm formation in desalination and water treatment plants. *Desalin. Water Treat.* 3, 136–142.
- Bar-Zeev, E., Berman-Frank, I., Stambler, N., Vázquez Domínguez, E., Zohary, T., Capuzzo, E., Meeder, E., Suggett, D.J., Iluz, D., Dishon, G., Berman, T., 2009b. Transparent exopolymer particles (TEP) link phytoplankton and bacterial production in the Gulf of Aqaba. *Aquat. Microb. Ecol.* 56 (2–3), 217–225.
- Berman, T., 2012. Transparent exopolymer particles as critical agents in aquatic biofilm formation: implications for desalination and water treatment. *Desalin. Water Treat.* <http://dx.doi.org/10.1080/19443994.2012.713585>.
- Berman, T., Mizrahi, R., Dosoretz, C.G., 2011. Transparent exopolymer particles (TEP): a critical factor in aquatic biofilm initiation and fouling on filtration membranes. *Desalination* 276 (1–3), 184–190.
- Buesing, N., Filippini, M., Bürgmann, H., Gessner, M.O., 2009. Microbial communities in contrasting freshwater marsh microhabitats. *FEMS Microbiol. Ecol.* 69 (1), 84–97.
- Coetser, S.E., Cloete, T.E., 2005. Biofouling and biocorrosion in industrial water systems. *Crit. Rev. Microbiol.* 31 (4), 213–232.
- Daims, H., Lückner, S., Wagner, M., 2006. Daime, a novel image analysis program for microbial ecology and biofilm research. *Environ. Microbiol.* 8 (2), 200–213.
- Darby, J.L., Attanasio, R.E., Lawler, D.F., 1992. Filtration of heterodisperse suspensions—modeling of particle removal and headloss. *Water Res.* 26 (6), 711–726.
- Eshel, G., Elifantz, H., Nuriel, S., Holenberg, M., Berman, T., 2012. Microfiber filtration of lake water: impacts on TEP removal and biofouling development. *Desalin. Water Treat.* 51 (4–6), 1043–1049.
- Flemming, H.C., 2002. Biofouling in water systems—cases, causes and countermeasures. *Appl. Microbiol. Biotechnol.* 59 (6), 629–640.
- Ityel, D., 2011. Ground water: dealing with iron contamination. *Filtr. Separat.* 48 (1), 26–28.
- Ives, K.J., 1982. Fundamentals of filtration. In: *Proceedings of the 21st European Federation of Chemical Engineering Event Symposium on Water Filtration, Antwerp, Belgium*.
- KLL, 2011. Annual Report of the Kinneret Limnological Laboratory. Israel Oceanographic and Limnological Research (IOLR). <http://www.ocean.org.il/Heb/ResearchInstitutesAndInfrastructure/LaboratoryResearchKinneret.asp>.
- Lane, D.J., 1991. 16S/23S rRNA sequencing. In: Stackebrandt, E., Goodfellow, M. (Eds.), *Nucleic Acid Techniques in Bacterial Systematics*. John Wiley & Sons, Chichester, England, pp. 115–175.
- Lee, N., Amy, G., Croue, J.P., 2006. Low-pressure membrane (MF/UF) fouling associated with allochthonous versus autochthonous natural organic matter. *Water Res.* 40 (12), 2357–2368.
- Mamane, H., Kohn, C., Adin, A., 2008. Characterizing shape of effluent particles by image analysis. *Separat. Sci. Technol.* 43 (7), 1737–1753.
- Mintz, D.M., 1966. *Modern Theory of Filtration*; International Water Supply Congress. Barcelona International Water Supply Association, London.
- Miura, Y., Okabe, S., 2008. Quantification of cell specific uptake activity of microbial products by uncultured *Chloroflexi* by microautoradiography combined with fluorescence in situ hybridization. *Environ. Sci. Technol.* 42 (19), 7380–7386.
- Momba, M.N.B., Kfir, R., Venter, S.N., Cloete, T.E., 2000. An overview of biofilm formation in distribution systems and its impact on the deterioration of water quality. *Water SA* 26 (1), 59–66.
- Mueller, L.N., de Brouwer, J.F.C., Almeida, J.S., Stal, L.J., Xavier, J.B., 2006. Analysis of a marine phototrophic biofilm by confocal laser scanning microscopy using the new image quantification software PHILIP. *BMC Ecol.* 6, 1.
- Newton, R.J., Jones, S.E., Eiler, A., McMahon, K.D., Bertilsson, S., 2011. A guide to the natural history of freshwater lake bacteria. *Microbiol. Mol. Biol. Rev.* 75 (1), 14–49.
- Nishimura, Y., Nagata, T., 2007. Alphaproteobacterial dominance in a large mesotrophic lake (Lake Biwa, Japan). *Aquat. Microb. Ecol.* 48, 231–240.
- Passow, U., 2002. Transparent exopolymer particles (TEP) in aquatic environments. *Prog. Oceanogr.* 55 (3–4), 287–333.
- Schloss, P.D., Westcott, S.L., Ryabin, T., Hall, J.R., Hartmann, M., Hollister, E.B., Lesniewski, R.A., Oakley, B.B., Parks, D.H., Robinson, C.J., Sahl, J.W., Stres, B., Thallinger, G.G., Van Horn, D.J., Weber, C.F., 2009. Introducing mothur: open-source, platform-independent, community-supported software for describing and comparing microbial communities. *Appl. Environ. Microbiol.* 75 (23), 7537–7541.
- Selje, N., Simon, M., 2003. Composition and dynamics of particle-associated and free-living bacterial communities in the Weser estuary, Germany. *Aquat. Microb. Ecol.* 30, 221–237.
- Sharma, D.K., King, D., Oma, P., Merchant, C., 2010. Micro-flow imaging: flow microscopy applied to sub-visible particulate analysis in protein formulations. *Am. Assoc. Pharm. Scientist* 12 (3), 455–464.
- Strathmann, M., Wigender, J., Flemming, H.C., 2002. Application of fluorescently labeled lectins for the visualization and

- biochemical characterization of polysaccharides in biofilms of *Pseudomonas aeruginosa*. *J. Microbiol. Methods* 50 (3), 237–248.
- Villacorte, L.O., Kennedy, M.D., Amy, G.L., Schippers, J.C., 2009. The fate of transparent exopolymer particles (TEP) in integrated membrane systems: removal through pre-treatment processes and deposition on reverse osmosis membranes. *Water Res.* 43 (2), 5039–5052.
- Yamada, T., Sekiguchi, Y., 2009. Cultivation of uncultured *Chloroflexi* Subphyla: significance and ecophysiology of formerly uncultured *Chloroflexi* 'Subphylum I' with natural and biotechnological relevance. *Microb. Environ.* 24 (3), 205–216.